



Cite this: *Dalton Trans.*, 2022, **51**, 12037

Received 6th July 2022,
Accepted 29th July 2022

DOI: 10.1039/d2dt02166h

rsc.li/dalton

We report, for the first time, the preparation and ionic conductivity of a Mg^{2+} -containing metal-organic framework (MOF) having type A features, *i.e.*, an anionic framework containing Mg^{2+} as the counter cation. We prepared $Mg_3[(MnMo_6O_{18})_2L]$ ($L^{12-} = C\{C_6H_4CH=NC(CH_2O)_3\}_4^{12-}$) (MOF-688-Mg) through a simple ion exchange reaction, and it showed high ionic conductivity above $10^{-5} \text{ S cm}^{-1}$ at 25°C under MeCN vapor.

Metal-organic frameworks (MOFs) have recently been developed as a new class of ionic conductor because of their designable architectures and porous structures, which allow us to introduce ionic carriers and to construct efficient ion-conducting pathways in their pores.^{1,2} So far, a lot of ion-conductive MOFs have been created by introducing various ionic carriers, such as protons,^{3–6} hydroxide ions,^{7,8} and lithium ions.^{9,10} However, there is a lack of reports on magnesium ion (Mg^{2+})-containing MOFs and their conductive properties, although Mg^{2+} conductors are of importance for application as the electrolyte of next-generation secondary batteries that do not require the use of rare elements such as lithium.¹¹

We have focused on creating novel Mg^{2+} conductors with MOFs by the introduction of Mg^{2+} carriers in their pores. Considering the charge compensation, there should be two possible ways to introduce Mg^{2+} carriers into the pores of MOFs.¹ The first is to introduce Mg^{2+} as the counter ion of the anionic framework (type A). The second is to introduce Mg^{2+} together with the counter anions, *i.e.*, the introduction of Mg^{2+} salts, which is applicable for charge-neutral or cationic frameworks (type B). So far, there are six reports of ionic conductivity of Mg^{2+} -containing MOFs, which are prepared by the introduction of Mg^{2+} together with counter anions (*i.e.*, type B features).^{12–17} However, there is no report of a Mg^{2+} -containing MOF with type A features and thus their ionic conductivity is

still unclear, even though type A features are expected to be the ideal structure for application as a battery electrolyte because of the high transport number and suppression of the side reaction of mobile anions. Here, in this study, we for the first time report the preparation of a Mg^{2+} -containing MOF with type A features through a simple ion exchange reaction with an anionic mother framework, MOF-688,¹⁸ and its ion-conductive properties. We clarified that the Mg^{2+} -containing MOF shows high ionic conductivity above $10^{-5} \text{ S cm}^{-1}$ at room temperature (RT) under a vapor of organic guest molecules.

The mother framework, MOF-688, $(NBu_4)_6[(MnMo_6O_{18})_2L]$ ($L^{12-} = C\{C_6H_4CH=NC(CH_2O)_3\}_4^{12-}$, NBu_4^+ = tetrabutylammonium), was synthesized by imine bond formation between $(NBu_4)_3[MnMo_6O_{18}\{O(CH_2)_3CNH_2\}_2]$ (abbreviated to $NBu_4\text{-Mn-Mo}_6$) and tetrakis(4-formylphenyl)methane (TFPM) (Fig. 1), according to a previous report (details are shown in

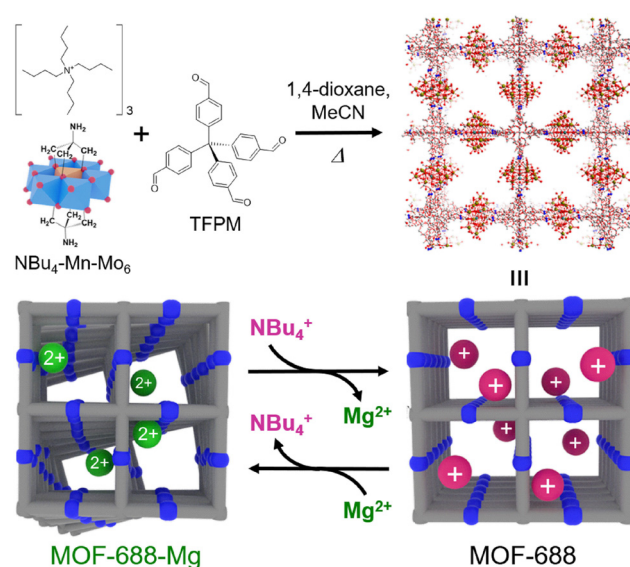


Fig. 1 Schematic illustration of the synthetic scheme of the Mg^{2+} -containing anionic MOF through an ion exchange reaction.

Department of Applied Chemistry, Faculty of Science Division I, Tokyo University of Science, 1-3 Kagurazaka, Shinjuku-ku, Tokyo 162-8601, Japan.

E-mail: sadakiyo@rs.tus.ac.jp

† Electronic supplementary information (ESI) available. See DOI: <https://doi.org/10.1039/d2dt02166h>



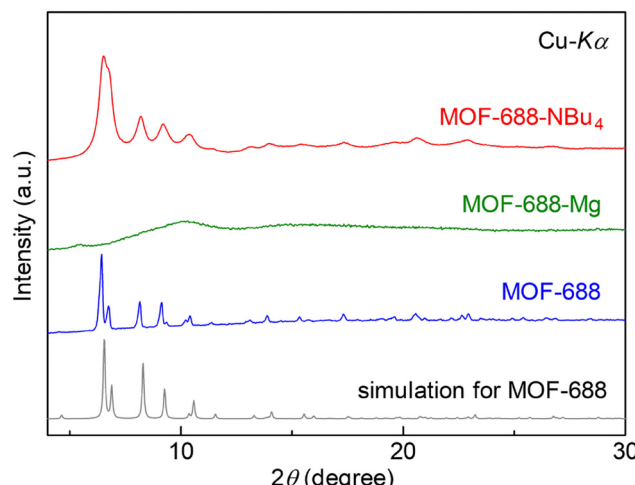


Fig. 2 XRPD patterns of MOF-688, MOF-688-Mg, and MOF-688-NBu₄.

the ESI[†].¹⁸ The successful synthesis of MOF-688 was confirmed by X-ray powder diffraction (XRPD) measurements (Fig. 2) and elemental analysis (ESI[†]). The included cations, NBu₄⁺, in MOF-688 were exchanged with Mg²⁺ through an ion exchange reaction; a powder sample of MOF-688 was immersed in a 1 M acetonitrile solution of Mg(TFSI)₂ (HTFSI = bis(trifluoromethanesulfonyl)imide) at RT for 5 days, followed by careful washing with pure anhydrous acetonitrile (immersed for 2 days) to remove the remaining Mg(TFSI)₂ from the sample (details are shown in the ESI[†]).

To confirm the existence of Mg²⁺ in the sample after the ion exchange reaction (MOF-688-Mg), we performed inductively coupled plasma atomic emission spectroscopy (ICP-AES) and ¹H-NMR measurements using a dissolved sample. From the results of the ICP-AES measurements, the number of Mg²⁺ ions included in MOF-688-Mg was estimated to be 2.9 per formula unit, confirming the stoichiometric ion exchange of NBu₄⁺ with Mg²⁺ to form MOF-688-Mg, Mg₃[(MnMo₆O₁₈)₂L]. As shown in Fig. S1,[†] the results of ¹H-NMR measurements clearly indicated the absence of NBu₄⁺ in MOF-688-Mg, which is consistent with the ICP-AES results. The results of elemental analysis also confirmed that the fundamental chemical composition of the framework was not changed after ion exchange (see the ESI[†]).

The XRPD pattern of MOF-688-Mg is shown in Fig. 2. The broadened peaks clearly indicated that MOF-688-Mg has an amorphous character. There should be two possibilities regarding the state of MOF-688-Mg. The first is that the framework structure of MOF-688-Mg completely collapsed during the ion exchange reaction, and thus it is not appropriate to call it a MOF sample. The second is that the ion exchange led to weakening of the long-range order of the framework, while the fundamental structure of the MOF still remained. To clarify this point, we reintroduced NBu₄⁺ to MOF-688-Mg through an ion exchange reaction (MOF-688-NBu₄) (see the ESI[†]). Reintroduction of NBu₄⁺ was confirmed by ICP-AES and ¹H-NMR measurements. From the results of the ICP-AES

measurements, there was no detectable amount of Mg²⁺ after the reintroduction of NBu₄⁺. In addition, there are apparent peaks from the reintroduced NBu₄⁺ in the ¹H-NMR spectra (Fig. S1[†]). These results clearly showed the successful ion exchange of Mg²⁺ with NBu₄⁺. The XRPD pattern of the prepared MOF-688-NBu₄ is shown in Fig. 2. The original patterns of MOF-688 were clearly recovered after the reintroduction of NBu₄⁺, indicating that MOF-688-Mg indeed has a MOF structure with weakened long-range order even after the incorporation of Mg²⁺ (Fig. 1). This is similar to the case with the introduction of Li⁺ into MOF-688.¹⁸ We also measured the IR spectra of the samples (Fig. 3). The absence of C-H stretching bands from NBu₄⁺ (at around 2870–2960 cm⁻¹) in MOF-688-Mg and the presence of them in MOF-688-NBu₄ confirmed the reversible ion exchange. Importantly, MOF-688-Mg showed characteristic peaks of the infinite framework of MOF-688, *i.e.*, C≡N stretching (at around 1640 cm⁻¹) and Mo–O–Mo stretching (at around 650 cm⁻¹), clearly confirming the presence of the remaining MOF structure in MOF-688-Mg. To the best of our knowledge, this is the first example of a Mg²⁺-containing MOF having type A features, prepared by a simple ion exchange reaction.

To elucidate the ionic conductivity of the Mg²⁺-included anionic MOF, we performed alternating current (ac) impedance measurements (Fig. 4 and S2[†]). We previously reported that the ionic conductivity of MOFs containing Mg²⁺ in their pores deeply depends on the outer environment, *i.e.*, gas or vapors of guest molecules.^{12,13} Thus, we measured the ionic conductivity under various environmental conditions, such as dry N₂ or organic vapors using a home-made sealed cell.¹² To eliminate the possibility of proton conduction, the measurements were performed after complete dehydration of the sample (see the ESI[†]). As shown in Fig. 4, the Mg²⁺-containing MOF did not show remarkable ionic conductivity under dry N₂ at ambient temperature. However, an apparent increase in ionic conductivity was observed under organic vapors and the

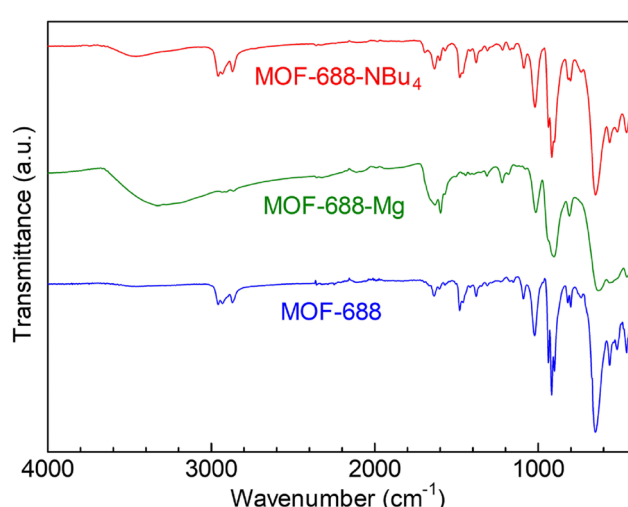


Fig. 3 IR spectra of MOF-688, MOF-688-Mg, and MOF-688-NBu₄.



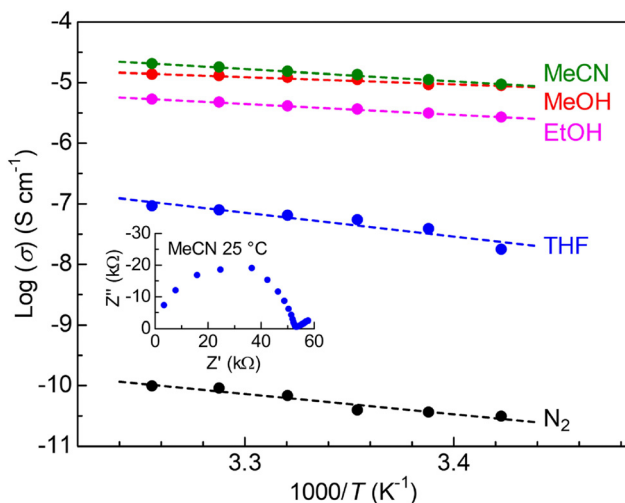


Fig. 4 The temperature dependence of the ionic conductivity of MOF-688-Mg under (black) dry N_2 or (green) MeCN, (red) MeOH, (pink) EtOH, and (blue) THF vapors. The inset shows an example of a Nyquist plot of the sample (25 °C, MeCN vapor).

MOF showed high ionic conductivity of $1.3 \times 10^{-5} \text{ S cm}^{-1}$ at 25 °C under MeCN vapor as the optimal guest. Considering that the possible ionic carrier is only Mg^{2+} located in the pores of the MOF, the drastic increase of ionic conductivity under the guest vapor should be derived from the increase of the mobility of Mg^{2+} . This is the first demonstration of vapor-induced ionic conduction of Mg^{2+} in a type A compound, although we previously reported vapor-induced ionic conduction in Mg^{2+} salt-containing MOFs (*i.e.*, type B compounds).^{12,13} This result clearly indicated that the mobility of aprotic ions such as Mg^{2+} can be enhanced by including guest molecules. To acquire information about the guest adsorption ability of MOF-688-Mg, we performed adsorption isotherm measurements. As shown in Fig. S3,† MOF-688-Mg adsorbed a considerable amount of MeCN at high vapor pressure, which reaches 3.3 molecules per formula unit (at 0.92 P/P_0), *i.e.*, 1.1 MeCN molecules per one Mg^{2+} . This clearly indicated that the MOF has the ability of MeCN vapor adsorption at RT, while the pore volume or pore size might be quite limited due to its interpenetrated structure,¹⁸ which was confirmed by almost no N_2 adsorption in MOF-688-Mg at 77 K (Fig. S4†). Compared to Mg^{2+} salt-containing MOFs (*i.e.*, Mg-MOF-74 $\supset \{\text{Mg}(\text{TFSI})_2\}_{0.15}$ and MIL-101 $\supset \{\text{Mg}(\text{TFSI})_2\}_{1.6}$),^{12,13} the adsorption amount of MOF-688-Mg for MeCN is relatively low and far from six molecules per Mg^{2+} , which is considered as the important number for the formation of coordinated Mg^{2+} species showing high mobility.^{12,13} Considering the fact that the ionic conductivity of the Mg^{2+} salt-containing MOFs (Mg-MOF-74 $\supset \{\text{Mg}(\text{TFSI})_2\}_{0.15}$: $2.6 \times 10^{-4} \text{ S cm}^{-1}$ (25 °C); MIL-101 $\supset \{\text{Mg}(\text{TFSI})_2\}_{1.6}$: $1.9 \times 10^{-3} \text{ S cm}^{-1}$ (25 °C))^{12,13} under optimal conditions is much higher than that of MOF-688-Mg, there seem to be two reasons for the limited conductivity of MOF-688-Mg. The first is the limited pore volume or pore size as mentioned above, which did not allow the included Mg^{2+} to

form highly mobile coordinated Mg^{2+} carriers due to the limited amount of guest adsorption. The second is the low crystallinity of MOF-688-Mg, which would prevent efficient migration of the formed carriers (*i.e.*, insufficient ion-conducting pathways). Table S1 shows the estimated activation energy (E_a) values of the samples. The relatively high activation energy of MOF-688-Mg (0.40 eV under MeCN) compared to the Mg^{2+} salt-containing MOFs (Mg-MOF-74 $\supset \{\text{Mg}(\text{TFSI})_2\}_{0.15}$: 0.26 eV (under MeOH); MIL-101 $\supset \{\text{Mg}(\text{TFSI})_2\}_{1.6}$: 0.18 eV (under MeCN))^{12,13} is also suggestive that the highly crystalline pores are one of the important factors for constructing efficient ion-conducting pathways in MOFs. These results suggest that anionic MOFs containing Mg^{2+} (*i.e.*, type A compounds) have great potential to be good Mg^{2+} conductors with optimal guests and that a highly crystalline anionic MOF with large-sized pores is one of the ideal structures for Mg^{2+} -conducting MOFs.

Conclusions

In conclusion, we synthesized a Mg^{2+} -containing MOF with type A features for the first time through a simple ion exchange reaction. This MOF showed high ionic conductivity of $1.3 \times 10^{-5} \text{ S cm}^{-1}$ at 25 °C under MeCN vapor because of the guest adsorption ability of the framework, while its crystallinity is low. We demonstrated that the Mg^{2+} located in the type A compound also showed a drastic increase of its mobility in the presence of organic guest vapors, which is similar to the case of Mg^{2+} salt-containing MOFs (type B compounds). These results should greatly contribute to the structural design and development of novel MOF-based Mg^{2+} conductors.

Conflicts of interest

The authors declare no competing financial interest.

Acknowledgements

This work was partly supported by the Nippon Sheet Glass Foundation for Materials Science and Engineering, the Takano Science Foundation, the Shorai Foundation for Science and Technology, the Kurata Grants by the Hitachi Global Foundation, the Tokuyama Science Foundation, JSPS KAKENHI No. 21K05089, and JST FOREST No. JPMJFR2110.

References

- 1 M. Sadakiyo and H. Kitagawa, *Dalton Trans.*, 2021, **50**, 5385–5397.
- 2 D.-W. Lim, M. Sadakiyo and H. Kitagawa, *Chem. Sci.*, 2019, **10**, 16–33.
- 3 J. M. Taylor, K. W. Dawson and G. K. H. Shimizu, *J. Am. Chem. Soc.*, 2013, **135**, 1193–1196.



4 W. J. Phang, H. Jo, W. R. Lee, J. H. Song, K. Yoo, B. Kim and C. S. Hong, *Angew. Chem., Int. Ed.*, 2015, **54**, 5142–5146.

5 M. Sadakiyo, T. Yamada, K. Honda, H. Matsui and H. Kitagawa, *J. Am. Chem. Soc.*, 2014, **136**, 7701–7707.

6 D. Umeyama, S. Horike, M. Inukai, T. Itakura and S. Kitagawa, *J. Am. Chem. Soc.*, 2012, **134**, 12780–12785.

7 M. Sadakiyo, H. Kasai, K. Kato, M. Takata and M. Yamauchi, *J. Am. Chem. Soc.*, 2014, **136**, 1702–1705.

8 S. S. Nagarkar, B. Anothumakkool, A. V. Desai, M. M. Shirolkar, S. Kurungot and S. K. Ghosh, *Chem. Commun.*, 2016, **52**, 8459–8462.

9 B. M. Wiers, M.-L. Foo, N. P. Balsara and J. R. Long, *J. Am. Chem. Soc.*, 2011, **133**, 14522–14525.

10 R. Ameloot, M. Aubrey, B. M. Wiers, A. P. G. Figueroa, S. N. Patel, N. P. Balsara and J. R. Long, *Chem. – Eur. J.*, 2013, **19**, 5533–5536.

11 H. D. Yoo, I. Shterengerg, Y. Gofer, G. Gershinsky, N. Pour and D. Aurbach, *Energy Environ. Sci.*, 2013, **6**, 2265–2279.

12 Y. Yoshida, K. Kato and M. Sadakiyo, *J. Phys. Chem. C*, 2021, **125**, 21124–21130.

13 Y. Yoshida, T. Yamada, Y. Jing, T. Toyao, K. Shimizu and M. Sadakiyo, *J. Am. Chem. Soc.*, 2022, **144**, 8669–8675.

14 S. Ma, L. Shen, Q. Liu, W. Shi, C. Zhang, F. Liu, J. A. Baucom, D. Zhang, H. Yue, H. B. Wu and Y. Lu, *ACS Appl. Mater. Interfaces*, 2020, **12**, 43824–43832.

15 E. M. Miner, S. S. Park and M. Dincă, *J. Am. Chem. Soc.*, 2019, **141**, 4422–4427.

16 S. S. Park, Y. Tulchinsky and M. Dincă, *J. Am. Chem. Soc.*, 2017, **139**, 13260–13263.

17 M. L. Aubrey, R. Ameloot, B. M. Wiers and J. R. Long, *Energy Environ. Sci.*, 2014, **7**, 667–671.

18 W. Xu, X. Pei, C. S. Diercks, H. Lyu, Z. Ji and O. M. Yaghi, *J. Am. Chem. Soc.*, 2019, **141**, 17522–17526.

